Tutors

Dr. Javier Tejero Salvador
Departament d'Enginyeria Química

Dra. Eliana Ramírez Rangel
Departament d'Enginyeria Química

Màster en Enginyeria Química

Treball Final de Màster

Screening of Acidic Ion-Exchange Resins to Produce Butyl Levulinate from Fructose and Butyl Alcohol

Selecció de resines àcides de bescanvi iònic per a produir levulinat de butil a partir de fructosa i alcohol butílic

Saúl Iglesias Prieto

February 2017

UNIVERSITAT DE BARCELONA

UNIVERSITAT DE BARCELONA

Screening of Acidic Ion-Exchange Resins to Produce Butyl Levulinate from Fructose and Butyl Alcohol

Saúl IGLESIAS PRIETO

Selecció de resines àcides de bescanvi iònic per produir levulinat de butil a partir de fructosa i alcohol butílic

Abstract

Alkyl levulinates are esters with the same boiling point as the lightest fraction of diesel fuel and can be obtained from lignocellulosic materials; therefore, introducing them in the formulation of commercial biodiesel fuels could potentially improve their properties. The aim of the present work is to perform a screening of acidic ion-exchange resins for their use as catalysts for the industrial production of butyl levulinate, taking butanol and fructose as raw materials.

Experiments were performed at 120 °C under 21.5 bar of pressure, working with reaction mixtures of 60 mL butanol, 10 mL water, 1.5 g fructose and 1 g catalyst. Resins with low DVB content were selected for the screening process, namely Amberlyst 31, Dowex 50WX2, Dowex 50WX4, Dowex 50WX8 and Purolite CT-124, all of them with a particle size of 100–200 mesh. Fructose conversions were around 95 % for Amberlyst 31 and CT-124, whilst Dowex resins reached roughly 100 %. The best performance was achieved with Dowex 50WX2, and Dowex 50WX4; the last one was finally chosen with a selectivity towards butyl levulinate of around 35 %.

The performance of the chosen resin was then studied at five different temperatures between 100 °C and 140 °C. Its yield towards BL decreased to 30 % at high temperatures, possibly due to the less stability of the ester in these conditions; lower temperatures, on the contrary, were discarded due to the slow reaction rate. The selected ideal temperature was therefore 120 °C.

Finally, the composition of the feed was changed by varying the fructose concentration (0.75 g and 3 g were tried). Higher concentrations produced severe darkening of the reaction mixture, revealing the formation of undesired by-products, dibutyl ether among them. Lower concentrations, on the other side, did not improve significantly the yield and resulted in overly dilute products. Consequently, a mass fraction of fructose around 2.5 % was deemed adequate. In these conditions, a yield towards the desired product of over 35 % was achieved, with fructose conversions of roughly 100 %.

Contents

List of Tables

List of Figures

List of Variables

Latin letters

- A – Area, area percentage, chromatographic reading
- C – Mass concentration, g/L
- M – Molecular mass, g/mol
- m – Mass, g
- $\hat{m}$ – Mass (measured, weighed, incomplete), g
- $\dot{m}$ – Mass contraction coefficient, g/h
- N – Number, amount, count
- n – Moles, amount of substance, mol
- $\bar{n}$ – Average number of moles, mol
- R – Molar ratio
- S – Selectivity
- s – Corrected sample standard deviation, mol
- t – Time, h
- V – Volume, mL
- $\hat{V}$ – Volume (measured, incomplete), mL
- $\bar{V}$ – Average volume, mL
- $\dot{V}$ – Volume contraction coefficient, mL/h
- w – Mass fraction
- X – Conversion
- x – Mole fraction

- Y – Yield
- ρ – Density, g/mL

Subscripts

- Bu – Butanol
- cat – Catalyst
- cyl – Graduated cylinder
- di – Dirty, unclean
- em – Empty
- fn – Funnel
- fr – Fructose
- fu – Full
- i – Generic replicate identifier
- j – Generic substance identifier
- rv – Reaction vessel
- sm – Sample
- T – Total (excluding catalyst)
- w – Water
- wg – Watch glass
- 0 – Initial

Pròleg

If the result confirms the hypothesis,
then you've made a measurement.
If the result is contrary to the hypothesis,
then you've made a discovery.

Enrico Fermi

El text que esteu llegint té un significat especial per a mi. Atès que el doctorat no es troba dins les meves intencions més immediates, aquest Treball Final de Màster constitueix el cim de la meva vida acadèmica, l'últim esforç després de gairebé vint-i-dos anys d'estudis. Vull que les meves primeres paraules siguin un agraïment a aquells que m'han ajudat a arribar fins aquí.

En primer lloc, gràcies als meus tutors, el doctor Tejero i la doctora Ramírez, que han demostrat una paciència infinita i han sabut transmetre'm els seus coneixements i els seus ànims durant els sis mesos que ha durat la meva convivència amb el grup de Catàlisi i Cinètica Aplicada. Gràcies també a la doctora Iborra pels seus sensats consells i les converses sobre la docència com a mode de vida. Tots tres m'han fet sentir com a casa meva. Voldria agrair també l'ajuda desinteressada dels meus companys de laboratori, Rodrigo Soto i Jordi Hug Badia, que m'han fet la feina més fàcil donant-me un cop de mà cada vegada que l'he necessitat. I gràcies a Ravi Sharma, que em va guiar durant els primers dies en el laboratori repetint-m'ho tot tantes vegades com ha calgut.

Gràcies als amics que m'heu acompanyat (encara ho feu) i que sou part de la meva vida, tant des de Santiago de Compostel·la com des de la Ciutat Comtal. Álex, Carla, Noe, Patri, Sonia, Ana, Any: m'identifico amb els vostres noms tant com amb el meu propi. Gràcies per ésser-hi sempre.

En últim lloc (el lloc d'honor), gràcies als meus pares i la meva germana. No només perquè, amb el vostre treball i esforç, hàgiu aconseguit que mai no m'hagi faltat res, sinó principalment perquè vosaltres m'heu creat. Em sento orgullós de la persona en què m'heu convertit, i crec que, d'una família, no se'n pot dir res millor. A vosaltres us dedico aquest treball. Us estimo.

1 Introduction

According to scientific data provided by NASA and NOAA (National Oceanic and Atmospheric Administration), 2016 was the hottest year ever recorded [1]. Even though individual yearly data are of little importance when referring to long-term phenomena like global warming, several unsettling trends have been observed, especially during the last century, that confirm the possibility of anthropogenic climate change with a very high degree of confidence.

The origin of these environmental issues is the intensification of the Earth's natural greenhouse effect, and the combustion of fossil fuels for transport and energy production is one of the main contributing factors to it. Thus attention towards this field has increased steadily during the last decades: the signature of the Kyoto Protocol in 1997 is only one example of the commitment of the international community to addressing these challenges.

1.1 Why renewable energies?

The concept of "renewable energy" applies to energy sources that are continually replenished by nature [2], preferentially on a human timescale. Even though this concept is often identified with "clean energy," these terms don't make reference to the same reality: nuclear power, which many people include among clean energies despite the residues that arise from its production, is clearly not renewable, since there is a finite amount of uranium in our planet. As will be seen, the opposite can also be true: there are renewable resources whose classification as "clean energies" might not be wholly satisfactory.

Mainstream technologies for the exploitation of renewable energy sources can be classified in the following categories:

- **Wind power.** Usage of airflows to run wind turbines, both on land and offshore.

- **Hydroelectric power.** This includes the exploitation of the kinetic energy of flowing streams, as well as waves (wave power) and tides (tidal power).
- **Solar energy.** The sun provides us with both light and heat. The former is exploited by photovoltaic systems, while solar thermal collectors and solar concentrators use heat.
- **Geothermal energy.** Usage of the heat generated inside the Earth to produce water steam, which is then led to a turbine.
- **Bioenergy.** Biomass, i.e. biological material (notably from lignocellulosic sources), can be processed to produce biogas and biofuels, which can then be burnt to obtain energy.

Indeed, most of the energy sources cited above are "clean energies," with the arguable exception of bioenergy, which still implies a combustion process.

Nevertheless, the environmental issues concerning fossil fuels are not the only reasons that advise a switch towards renewable energies. The fact that fossil fuels themselves (mainly coal, petroleum and natural gas) are non renewable implies that they will eventually become depleted or too scarce to be profitable. In addition to that, fossil fuels are not uniformly distributed in the Earth's crust, which means that petroleum-consuming countries are often economically dependent on the extraction policies of petroleum-exporting countries.

All these considerations have led not only to the signature of the Kyoto Protocol, but also to the approval of several national and international laws promoting the research on renewable energy sources and their responsible consumption. At the European level, this concern is reflected in the adoption of the *Directive 2009/28/EC of the European Parliament and of the Council, of 23 April 2009, on the promotion of the use of energy from renewable sources and amending and subsequently repealing Directives 2001/77/EC and 2003/30/EC.* This Directive confirmed a target of at least a 20 % share of energy from renewable sources in the Community's gross final consumption of energy and a 10 % share of the final consumption of energy in transport in 2020.

1.2 Why biofuels?

The aforementioned Directive draws especial attention to the use of biofuels. Around one third of the energy consumption in the European Union is destined to transport, according to Eurostat [3], and the US Environmental Protection Agency states that this sector generates a quarter

of the greenhouse gas emissions in that country [4]. This is a field where the use of "clean energies" *stricto sensu,* that is, excluding biomass, is still under development and, in many cases, not yet actually cost-effective. According to the European authorities, burning biomass and biofuels might be, although not strictly *clean,* the best bid to achieve a realistic short-term reduction of carbon emissions, as required by EU policies.

Biofuels can be classified in three generations according to their origin. **First-generation biofuels** are produced from classic food crops (using seeds, grains or sugars as substrates) with cheap, well-known technologies; consequently, they are readily available and of widespread use in several countries. Nevertheless, the main drawback of first-generation biofuels is that their production can (and, in fact, do) compete with food crops, thus placing a high stress on food commodities [5].

To overcome these disadvantages, **second-generation biofuels** can be derived from non-food crops, preferably from lignocellulosic biomass. The main problem with this class of biofuels is that they require a pre-treatment of the lignocellulosic material for the obtention of sugars thereof. This pre-treatment is usually expensive: economic analyses indicate that the process of sugar release (including pre-treatment, enzyme production and enzymatic hydrolysis) contributes to as much as 45 % of the projected total cost [6].

There also exists a category of **third-generation biofuels** derived from algal biomass which allegedly overcomes many of the disadvantages of first- and second-generation biofuels, such as the non-existent competition with agricultural food and feed production and its increased hydrolysis or fermentation efficiency [7]. Nevertheless, much more research is needed for this technology to be considered even potentially cost-effective.

1.3 Why butyl levulinate?

So far, the traditional method for increasing the share of biofuels in transport fuels has been the direct addition of bioethanol in commercial diesel fuels. However, bioethanol-diesel blends are not satisfying: ethanol decreases the cetane number, fuel viscosity and mixture stability of commercial blends [8]. Two alternatives remain: the use of bioethanol not as a pure additive, but as an ethylating agent to give oxygenated compounds, or else the choice of new compounds that are readily available from lignocellulosic biomass.

In this field, attention has been drawn to alkyl levulinates derived from biomass, especially to ethyl levulinate [9]. Ethyl levulinate blending does not create any negative impact on the

volatility of diesel fuel and may not require any modification of existing engine designs [10]. Additionally, levulinic acid can be obtained from biomass, which qualifies it as a biofuel. These reasons, among others, have led the United States Department of Energy to identify levulinic acid as a promising building block for chemistry [11].

The properties, production and performance of both methyl (ML) and ethyl levulinates (EL) have been widely studied. Comparatively, the potential of butyl levulinate (BL or, according to IUPAC, butyl 4-oxopentanoate) has been left untapped [5]. The properties that make EL desirable for its inclusion into diesel blends are also shared by BL (viz. a reduction in the vapour pressure of the blend, a freezing point lower than -60 °C, better cold-flow properties of the resulting blend, and acceptable boiling and flash points, lubricity and conductivity). Additionally, BL remains completely soluble in diesel fuel down to its cloud point (around -25.8 °C) [9]. This makes BL even more promising than EL [5], even though both have low cetane numbers.

1.4 Alternative applications of alkyl levulinates

Alkyl levulinates have additional potential applications thanks to their properties [12]. The use of levulinates as green solvents has been proposed due to their similar characteristics but lower vapour pressures than usual solvents. Another important field of application of alkyl levulinates concerns their transformation into γ-valerolactone, which can itself be found in the perfumes and food industries or as a fuel additive.

2 State of the art

Historically, the first successful attempts to synthesise alkyl levulinates are documented as soon as 1877 [13], using **levulinic acid** directly as a raw material. Forty years later, Sah [14] and Schuette [15] reported the formation of several alkyl levulinates, with BL among them, in the corresponding alcohol in presence of hydrochloric acid as a catalyst. Different standpoints and methods of production have appeared and evolved ever since, as will be discussed in this Chapter.

2.1 Raw materials

The first decision that has to be made when addressing the study of BL production is what the starting point of the reaction will be. The most intuitive choice might initially be the immediate predecessor of BL, levulinic acid (and so has historically been), but several other possibilities exist.

2.1.1 Levulinic acid

As it has already been mentioned, levulinic acid (LA) was the first reagent considered for the obtention of alkyl levulinates. It has been observed that LA undergoes an esterification reaction with alcohols in both catalysed and non-catalysed environments at mild (or even at room) temperatures [16]. Most experiments have focused on ML and, especially, EL [12], but some have reached BL [5, 17] or even higher-molecular-mass esters [18]. Yields were often above 90 %.

Even though this reaction is rather straightforward, as can be seen in Figure 2.1, LA might not be the most adequate choice as a raw material. The fact is that LA is a compound with an

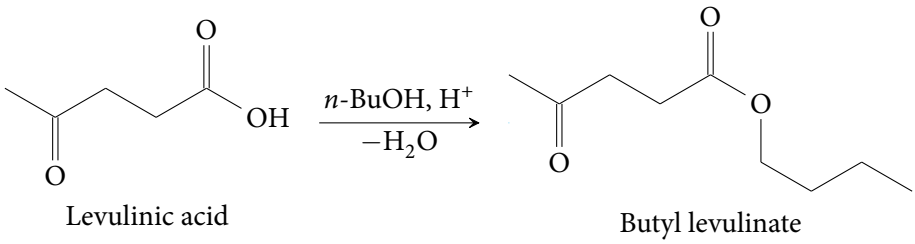

Figure 2.1: Acid-catalysed esterification reaction of LA [5].

already high added value, which can result in a loss of profitability of the process. Furthermore, since LA is ultimately obtained from biomass, the possibility of skipping LA as an intermediate compound and producing the desired ester directly from lignocellulosic materials should also be taken into consideration.

2.1.2 Polysaccharides and biomass

The possibility of obtaining alkyl levulinates directly from lignocellulosic biomass through an integrated process is certainly seductive. Abundant research has been carried out using refined powder **cellulose** as a raw material [12], the first experiments dating from 1988 [19]. Nevertheless, when shifting towards more complex lignocellulosic materials such as **wood,** grass or straw, yields drop dramatically to a range between 17 % and 37 % in weight.

Not only is the decomposition of hard, complex biomass difficult, but it also generates a wide range of undesired by-products, many of which can be classified as **humins:** organic compounds of high molecular weight, insoluble in water, formed by polymerisation of smaller organic molecules. The formation of humins poses a threat to the smooth performance of the reaction, fouls the equipment and implies a loss of carbon that would otherwise evolve towards the desired product [20].

2.1.3 Monosaccharides

This work will focus on the use of monosaccharides, namely **D-fructose**, as a raw material for the synthesis of BL. Monosaccharides seem an interesting choice when aiming to start as back in the reaction scheme as possible, but not wanting to cope with the problems intrinsically associated with lignocellulosic biomass.

The most studied monosaccharides are glucose (an aldohexose) and fructose (a ketohexose). Glucose is reportedly less reactive than fructose; even though these isomeric reactants do not

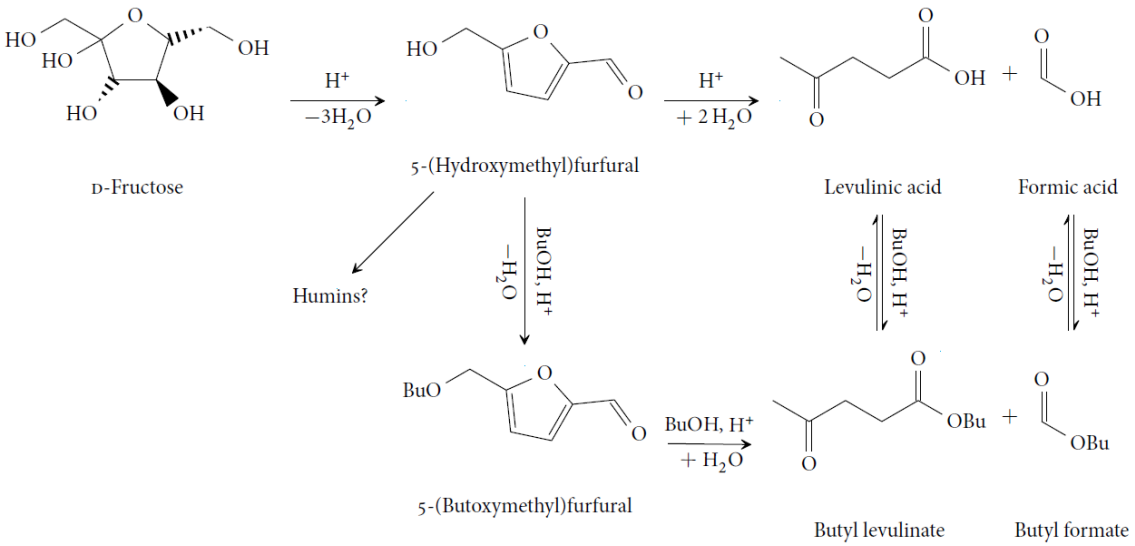

Figure 2.2: Reaction routes for BL production from D-fructose [10, 12].

show a great difference in conversion [12], the yield has been observed to be significantly reduced when fructose is replaced by glucose [10]. This might be due to the presence of side reactions (e.g. polymerisation) during the isomerisation of glucose to fructose [21]. Other monosaccharides have also been studied, such as xylose [22], mannose [23], sorbose [23] or galactose [21], albeit much less thoroughly.

The scheme of reaction routes from fructose to BL is not simple. A proposed reaction path is shown in Figure 2.2.

2.2 Catalysts

If fructose and butanol are let to react freely, hardly any progress is reported in the esterification reaction, if any at all.[(1)] Therefore, a suitable catalyst is necessary for the chain of reactions to progress.

2.2.1 Homogeneous catalysts

In the field of BL synthesis, homogeneous catalysts have traditionally been used. Hydrochloric acid was the first one to be employed [14, 15]; since then, others have also been researched, e.g.

[(1)] *infra* 5.1.

phosphoric acid H_3PO_4 and sulphuric acid H_2SO_3 [5]. Nevertheless, the use of homogeneous catalysts has got some drawbacks.

One problem, which is common to all homogeneous catalysts, is that a separation stage is necessary after the reaction stage in order to recover the catalyst from the final mixture. Usually, this separation consists on a distillation, which is frequently expensive. Additionally, it has been observed that the alcohol undergoes a dehydration process when the acid concentration is too high, giving place to dialkyl ether [12]. This undesired reaction is only prevented by working at very low acid concentrations, in the order of a few millimoles per litre [24]. Equipment corrosion and environmental issues also arise with mineral acid [25].

2.2.2 Heterogeneous catalysts

The problems with homogeneous catalysts have led to an ever increased research on heterogeneous catalysis. Different types of solid catalysts have been tried, some of which can be seen in Table 2.1. Zeolites have got many advantages, but they are not hydrothermally stable in water during the reaction, which leads to a loss of structural integrity and can, therefore, not be recycled. Montmorillonite-based catalysts have also been investigated, but experiments resulted in low selectivity towards levulinic acid and a large amount of humins [29]. More exotic materials, such as heteropoly acids (namely silicotungstic and phosphotungstic acids) and sulphonic-acid-functionalised carbon nanostructures, have also been tried.

Contrastively, acidic ion-exchange resins have been hardly investigated as heterogeneous catalysts for the production of BL. Some experiments have been performed to obtain BL directly from LA using gel-type poly(styrene-*co*-divinylbenzene) resins (PS-DVB resins) [5]. Some monosaccharides have also been treated with this type of catalysts: fructose with ethanol [25], glucose with methanol [28] and several other such as xylose, galactose or levoglucosan [10], although none of them with butanol.

Table 2.1: Catalytic materials, reaction conditions and yield of monosaccharide alcoholysis.

Substrate	Alkyl	Catalyst	T / °C	t / min	Y_{mol}	Ref.
fructose	Et	H-USY zeolite	160	1 200	40 %	[23]
fructose	Me	sulphonated titania, TiO_2-SO_3H	200	120	59 %	[26]
fructose	Et	poly(*p*-styrenesulphonic acid)-grafted nanotubes	120	1 440	84 %	[25]
fructose	Et	acidic ion-exchange resin, Amberlyst-15	120	1 440	73 %	[25]
fructose	Bu	silicotungstic acid, $H_4SiW_{12}O_{40}$	140	900	60 %	[27]
glucose	Me	acidic ion-exchange resin, Amberlyst-70	170	180	90 %	[28]

Sulfonated PS-DVB resins have become more and more important since the end of World War II. Several industrial applications have been found suitable for them; the synthesis of methyl-*tert*-butyl ether (MTBE) is by far the most important one, but this kind of resins are also used to produce isopropanol, bisphenol A or but-1-ene oligomers, for example [30].

2.2.3 Insight into ion-exchange resins

The field of ion-exchange resins, also called organic cross-linked functional polymers or OCP's, is becoming increasingly attractive to industries and researchers thanks to the advantageous characteristics of this kind of catalyst. In addition to the features that are common to all heterogeneous catalysts (viz. insolubility, facile separation, easy handling, etc.), polymeric supports have many other interesting properties [31]: they are usually nonvolatile, nontoxic and often recyclable, properties that are especially attractive in an era of enhanced environmental awareness.

Ion-exchange resins are normally divided in two main categories attending to the basic morphological characteristics of the catalyst: microporous and macroporous. Their main features are [30]:

- Microporous or **gel-type resins** have got no appreciable porosity when dry, wholly depending on swelling in the reaction medium to render their interior accessible.
- Macroporous or **macroreticular resins** possess stable macropores even in the dry state. However, they also undergo swelling in the reaction environment, generating additional micropores.

The polymeric matrix of OCP's is formed by hydrocarbon chains entangled with one another by a cross-linking agent, providing a hydrophobic 3D structure. The manufacturing processes of both types of resins are very similar. Initially, a homogeneous mixture of styrene and divinylbenzene is dispersed as small droplets in an aqueous phase. This mixture will include a porogenic agent for the formation of macroreticular resins, with cross-linking degrees exceeding 8 % needed, whilst no porogenic agent is required for gel-type resins. The morphological structure of the resulting catalyst can vary widely depending on the polymerisation conditions [30].

Once the polymeric matrix is formed, the polymer has to be functionalised, thus turning its structure hydrophilic. This can be achieved with various procedures; sulphonated materials are

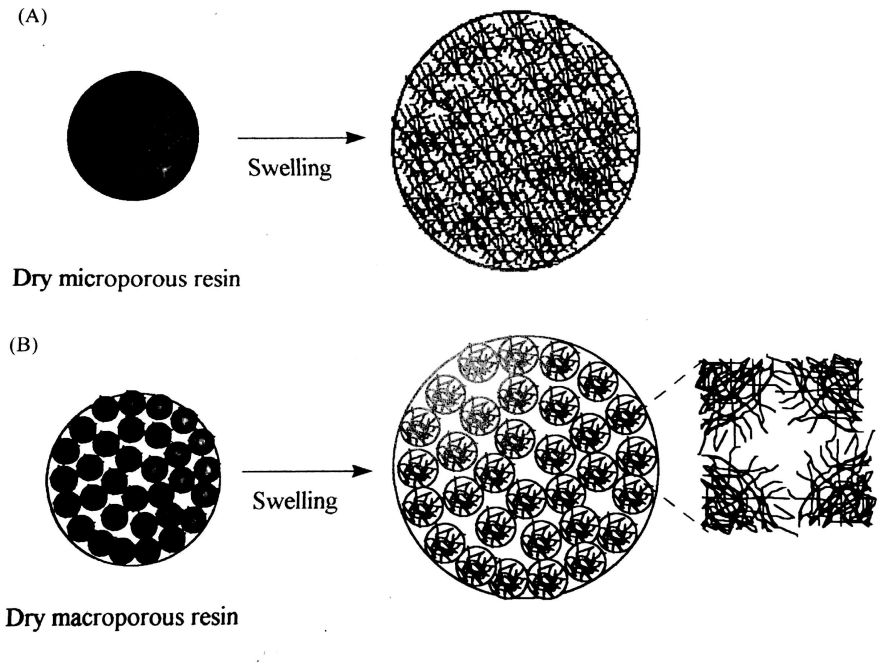

Figure 2.3: Schematic representation of changes in the morphology of polymeric resins during swelling. Figure A shows a gel-type polymer bead, whilst figure B shows a macroreticular polymer bead [30].

nearly exclusively prepared by direct sulphonation of polystyrene with concentrated sulphuric acid. Basic resins for anion exchange are also commercially available, but they are thermally unstable over 60 °C and they deactivate easily by carbon dioxide present in air.

The phenomenon of **swelling** is critical for the performance of PS-DVB resins. In a typical macroreticular resin, 95 % of all the acidic active centres are accessible only when the polymer mass opens additional porosity after swelling in the reaction medium. Figure 2.3 offers a schematic representation of changes in the morphology of polymeric beads during swelling [30].

It is understandable that a deep insight of the internal morphology of the resins in their swollen state will be of paramount importance. The best technique currently in use to assess the nanomorphology of swollen resins is inverse steric-exclusion chromatography or ISEC. This technique consists on eluting solutes of known molecular size through a stationary phase composed by the swollen polymer to be studied.

3 | Objectives

There is a considerable lack of scientific literature concerning the production of BL from fructose using acidic gel-type PS-DVB resins. A preliminary insight has been provided by SHARMA [32], who studied the different performance of gel-type vs. macroreticular resins for this process, as well as a shallow assessment of the effect of catalyst mass and reaction temperature. This study found that gel-type resins performed better than macroreticular resins; therefore, only gel-type (microreticular) resins will be investigated in this work.

In particular, the specific objectives of this Master's Thesis will be:

1. A study of the performance of different acidic gel-type PS-DVB resins for the reaction object of this work.
2. A selection of the best resin, with basis on catalytic criteria (conversion and selectivity towards the ester).
3. An optimisation of the reaction temperature for the selected catalyst.
4. An optimisation of the feed composition for the selected catalyst, at the selected reaction temperature.

4 Experimental procedure

4.1 Materials

The materials that have been used throughout this research will be classified according to the experimental stage in which they were employed.

4.1.1 Reactants and catalysts

The reaction mixture of the experiments consisted on **butan-1-ol** (99.5 %, Acros Organics), **ultrapure water** (Milli-Q, Millipore Corp.) and **D-(–)-fructose** (99 %, Labchem). The pressurisation of the reactor was done with **nitrogen** (99.99 %, Abelló Linde).

Acidic ion-exchange PS-DVB sulphonated resins were used as catalysts throughout the experiments. The resins selected were **Amberlyst™ 31** (Rohm and Haas, henceforth A31), **Purolite® CT124** (Purolite, henceforth CT124), **Dowex® 50WX2** (Sigma-Aldrich, henceforth DOW2), **Dowex® 50WX4** (Sigma-Aldrich, henceforth DOW4) and **Dowex® 50WX8** (Sigma-Aldrich, henceforth DOW8). All resins were supplied wet and in hydrogen form. Their properties can be seen in Table 4.1.

The main reason why these catalysts were selected for the screening stage is that compounds with great molecular mass will be present in the process, including BL and 5-BMF. According to previous experimental evidence, the formation of these compounds is favoured by resins with high swelling capacity, thus putting gel-type catalysts under the spotlight. SHARMA [32] investigated DOW2 and DOW4; therefore, DOW8 was also selected in order to have a global perspective of the whole catalyst family. A31 and CT124 were selected for their similar internal structure.

Table 4.1: Properties of acidic ion-exchange resins used in this work.

	A31	DOW2	DOW4	DOW8	CT124
Acid capacity (meq/g)	4.80	4.83	4.95	4.83	5.00
Divinylbenzene (%)	4	2	4	8	4
Particle diameter (μm)	469	106	106	116	771
Water retention as shipped (%)	63–67	74–82	64–72	50–58	60–65
Maximum temperature (°C)	130	150	150	150	130
Swelling in butanol (%)	40.8	45.6	43.7	32.2	43.8
Swelling in water (%)	51.3	58.6	54.8	20.5	53.7

4.1.2 Auxiliary substances for analysis

The analysis of the reaction product mixture was performed by a combination of gas chromatography (GC) and high-performance liquid chromatography (HPLC). For GC, **helium** (99.99 %, Abelló Linde) was used as the carrier gas. For HPLC, the mobile phase was a dilute solution of sulphuric acid elaborated by dilution of a commercial **sulphuric acid solution** (0.05 M, Fisher Chemical) with **water** (Milli-Q, Millipore Corp.).

For the chromatographic calibrations, the reagents used were **butan-1-ol** (99.5 %, Acros Organics), **levulinic acid** (98 %, Acros Organics), **formic acid** (98 %, Labkem), **butyl formate** (98 %, Acros Organics), **butyl levulinate** (98 %, Sigma-Aldrich), **5-(hydroxymethyl)furfural** (98 %, Acros Organics) and **dibutyl ether** (99 %, Acros Organics).

4.2 Equipment

4.2.1 Reactor setup

The experiments were carried out in a 100 mL stainless-steel batch reactor (Autoclave Engineers 316 SS) with a working overpressure of 21.5 bar. The reactor, whose diagram can be seen in Figure 4.1, consists on a stirring system, a relief valve, a manometer and a rupture disc. The stirring system includes a four-bladed axial-up propeller mounted on a Magnedrive II Series 0.7501 rotor. The stirring speed is controlled through a frequency converter T-Verter N2 Series. A 316 SS baffle is located alongside the axis of the propeller, parallel to it, in order to break possible vortices generated by the stirring. This makes the flux regime closer to an ideal mixed-flow

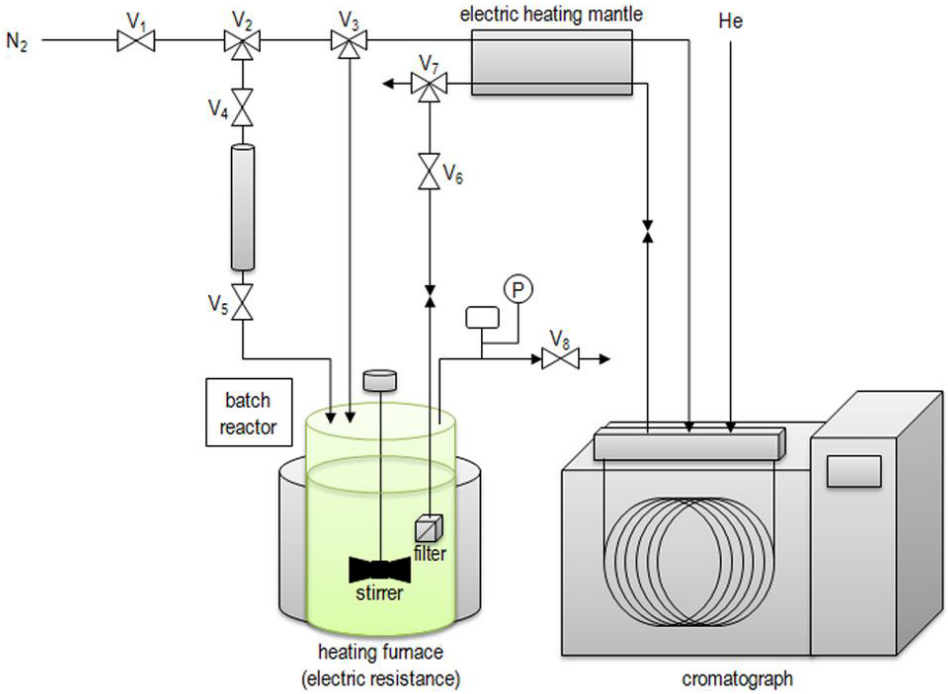

Figure 4.1: Diagram of the experimental setup [33].

model. A type-K (chromel-alumel) thermocouple, belonging to a PID temperature control system, is also located alongside the turbine axis to measure the temperature inside the reactor. Sampling takes place through a sintered-iron filter with a mesh size of 0.5 µm.

Pressure measurements are taken through a Labon CB6020 pressure transducer. Pressure reads are made visually through a Bourdon pressure gauge located above the reactor. The rupture disc can stand a pressure of 50.1 bar to 54.8 bar with a 5 % error margin.

The heating system is composed by an electric heating furnace TC-22 Pro 9 controlled by the reactor's internal temperature and that of its external wall, both measured using thermocouples. The error margin of the system, once the setpoint is achieved, is of ±0.1 °C.

The catalyst is injected through a 316 SS tube. The desired amount of catalyst is propelled with nitrogen thanks to the pressure difference between the gas supply and the interior of the reactor.

The samples were collected into 2 mL wide-opening screw-top vials from Agilent, made of borosilicate glass.

Two balances were used for the measurement of masses: an AND HR120 analytical balance with a readability of 0.1 mg (although readings were rounded up to the nearest milligramme) and a Denver Instrument SI-4002 balance with a 10 mg precision.

4.2.2 Gas chromatography

The GC analysis has been performed in a Hewlett–Packard 6890 GC system with an HP-PONA 19091S-001 column with a dimethylpolysiloxane stationary phase. The column is 50 m long and has got a 200 μm diameter, the stationary phase being 0.5 μm thick. The samples were introduced in the system using a 1.0 μL Agilent syringe.

4.2.3 High-performance liquid chromatography

The HPLC analysis has been performed in an Agilent 1260 Infinity Quaternary LC system with an Agilent Hi-Plex H column for organic acids. The column is 300 mm long and has got a 7.7 mm diameter, the stationary phase consisting on monodisperse, sulphonated PS-DVB particles with a particle size of 8 μm. The samples were introduced into the system by means of a 50 μL Agilent syringe.

4.3 Procedure

4.3.1 Catalyst pretreatment

As can be seen in Table 4.1, the ion-exchange resins in use in this work are highly hygroscopic and, as such, tend to absorb water from air very easily; in fact, many of them are supplied "wet" by the manufacturer. This water can contribute to resin inhibition. Consequently, water was always removed from the catalysts before use.

The drying process consisted on two steps: a mechanical drying process in an oven at atmospheric pressure and 110 °C for a minimum of 2 h, and a vacuum drying process at 10 mbar and 100 °C overnight.

Additionally, not all of the resins have got the same particle diameter (v. Table 4.1). More specifically, A31 and CT124 are much coarser than Dowex® resins. For them to be comparable, these resins were dried, ground and sieved and the size fraction between 80 μm and 100 μm was used. This size fraction was then subjected to a new drying process.

4.3.2 Reactor loading

The reaction mixture was produced directly in the stainless-steel reactor. The process consisted on measuring 60 mL of butan-1-ol and 10 mL of water in a graduated cylinder, then carefully adding them into the reaction vessel, weighing the desired amount of D-fructose in an analytical balance and adding it to the reactor as well. Several measures were taken throughout the process so as to know exactly the proportion of each substance in the final mixture:

- The reaction vessel was weighed twice, empty first and then full after all the substances were added.
- The graduated cylinders were weighed twice, full first and then empty after pouring their content into the reaction vessel.

The reaction vessel was then mounted in place, a rubber gasket was added to ensure hermeticity and the reactor was secured with three retaining bolts. Then valve 1 was opened for the nitrogen to get in and valve 3 was set at position 2. When an overpressure of 21.5 bar was achieved, valve 3 was once again set at position 1 and the heating furnace was placed around the reactor and fastened properly.

4.3.3 Experiment launching

The stirring system was activated at 500 rpm and the electric heating furnace was switched on. Its surface temperature setpoint was programmed 30 °C above the desired temperature.

Whilst the heating of the reaction system, the computer controlling the GC was started and the Chemstation software was loaded. The HPLC was set to a flow rate of 0.6 mL/min, closing the recycling and purge valves, in the OpenLAB software. The maximum flow gradient was set at 0.1 mL/min^2 so as to make sure that all changes in the flow rate are made smoothly.

Afterwards, the vacuum of the drying furnace was broken and the desired mass of catalyst was measured with an analytical balance. The catalyst was then introduced into the injector chamber by means of a funnel. Several measures were taken throughout the process so as to know exactly the amount of catalyst added, considering that a small amount of catalyst can adhere to the glassware: the funnel and the watch glass used to weigh the catalyst were themselves

weighed twice (firstly, after the catalyst was introduced into the injection chamber and some amount of catalyst was still adhered to them, and secondly, after they were cleaned up).

When the reaction mixture attained the desired temperature, the catalyst was injected. Valve 8 was opened for the pressure in the reaction vessel to decrease, then closed; valve 2 was opened to redirect the nitrogen towards the injector and valves 4 and 5 were consecutively opened for the catalyst to enter the reaction chamber. Then valves 5, 4 and 2 were closed in that order. All this process was repeated twice more in order to ensure that no catalyst remains in the injection chamber.

The reaction can then be considered to have begun. The instant of the catalyst injection is identified with the initial reaction time, t_0.

4.3.4 Sampling

The sampling procedure consisted on setting valve 3 in position 2, opening valve 6 and then slowly and carefully opening valve 7 to collect the sample into a vial. Approximately 0.5 mL samples were collected. Once the sample had been taken, valves 7 and 6 were closed back and valve 3 was set into position 1.

At this point, some liquid may remain inside the piping. In order to redirect it back into the reaction vessel, valve 8 was opened to lower the pressure in the reactor, then closed, and valve 6 was opened to propel the remaining liquid into the reactor, then closed. This procedure was repeated twice more. Finally, valve 7 was purged.

Samples were usually taken after 30 min and 60 min of reaction, and then every hour until the end of the experiment.

4.3.5 Sample analysis

For the GC analysis, after the sample data were entered into the software, the syringe was charged with the sample several times to prevent foreign substances to enter the chromatograph. Afterwards, 0.1 µL were measured and injected into the chromatograph, then pressing the START button. After 0.30 s, the syringe was extracted from the chromatograph and cleaned several times with acetone. The analysis lasted roughly 25 min.

On the other side, for the HPLC analysis, 50 µL of sample were charged in the syringe and injected into the chromatograph twice, in order to ensure that the injection loop is fully loaded with the sample. After the sample data were entered into the software, the analytical method was started and the valve turned to the INJECT position. The syringe was left inserted until the appearance of the first peaks on the chromatogram; it was then extracted and washed with acetone and water. After 50 min approximately, when the peak corresponding to butan-1-ol appeared, the analysis had to be manually stopped.

4.3.6 Clean-up

After the last sample was collected, the heating and stirring systems were switched off, valve 1 was closed to prevent the nitrogen from entering the system and valve 8 was opened to alleviate the pressure. The heating furnace was then removed carefully and the reactor was left to cool down. Once the reactor reached ambient temperature, the three retaining bolts were unscrewed and the full reactor vessel was weighed to determine the mass loss during the reaction. The product mixture was then filtered to recover the catalyst.

Once empty, the reactor was washed with water and acetone and dried with synthetic air. The filter was unscrewed from its support, submerged in hexane in a beaker and placed in an ultrasonic bath for 25 min, then dried with synthetic air and put back in place.

4.4 Experimental conditions

Eight-hour experiments were carried out at 21.5 bar and at temperatures between 100 °C and 140 °C. Relatively high temperatures were chosen (albeit milder than in other experiments in the bibliography[(1)]) because, as shown by previous experiments [32], BL forms at temperatures above 100 °C. Additionally, given that most resins cannot stand temperatures above 150 °C,[(2)] this temperature was never reached during the experiments.

However, working at high temperatures implied that the reaction mixture would partially or totally volatilise, since butan-1-ol boils below 120 °C. High pressures prevented the reaction mixture from volatilising, but they had also got other advantages: the circulation of liquid

[(1)] V. Table 2.1.
[(2)] V. Table 4.1

inside the piping was made easy due to mere pressure gradients, and the injection of the catalyst inside the reaction vessel was also done thanks to this wide pressure difference.

The experiments have been performed with a ternary mixture of water, butan-1-ol and fructose. The presence of water is justified, even though it can favour the formation of undesired by-products, because glucose is insoluble in the pure alcohol. The molar ratio between butan-1-ol and water was always $R_{\mathrm{Bu/w}} \approx 1.19$. These proportions are based on the previous literature [32]. This ratio is low enough for the mixture to fall outside the insolubility bell of the water–butan-1-ol mixture, even taking into account possible temperature variations [34]. It is also inside the solubility region of the D-fructose–water mixture [35, 36]. Some data do exist for the water-butanol-fructose ternary system [37], but only at room temperature. Nevertheless, an experiment was performed to test the solubility of this system at higher temperatures. A mixture containing 2 g D-fructose, 20 mL water and 120 mL butan-1-ol became soluble above 60 °C at atmospheric pressure. When the amount of D-fructose was doubled, the mixture became soluble above 90 °C. Therefore, the reaction mixture can be considered to be completely homogeneous in the conditions of the experiment.

In total, 25 experiments were performed. Nevertheless, some of them were just replicates in the same experimental conditions in order to determine the experimental error, and others were later deemed invalid. A list of the valid experiments and their experimental conditions can be seen in Table 4.2.

4.5 Calculations

The mathematical calculations that were performed for all the experiments are analogical and can be illustrated with an example. With that purpose, the calculations performed during the experiment no. 15 will be detailed in this Section.

4.5.1 Initial quantities

During the reactor loading step, all measures taken were recorded in a table specially designed for that purpose. Table 4.3 reflects that model for the experiment no. 15. With those data, the following quantities can be calculated:

- Initial mass of butan-1-ol: $m_{\mathrm{Bu},0} = m_{\mathrm{Bu,cyl,fu}} - m_{\mathrm{Bu,cyl,em}}$

Table 4.2: List of experiments performed throughout this work and their experimental conditions.

Exp. ID	Catalyst	m_{cat} / g	T / °C	m_{fr} / g	t / h
4	DOW2	0.99	120	1.50	6
5	DOW8	0.96	120	1.50	6
7	DOW4	0.95	120	1.51	8
8	DOW2	0.95	120	1.50	8
9	DOW4	1.71	120	1.50	8
10	DOW4	1.90	120	1.51	8
11	CT124	1.02	120	1.50	8
12	A31	0.97	120	1.51	8
13	DOW2	0.96	120	1.50	8
14	DOW4	0.99	120	1.51	8
15	DOW4	0.98	120	1.50	8
16	DOW4	0.49	140	1.50	8
17	DOW4	1.96	110	1.51	8
18	DOW4	0.50	130	1.50	6
19	DOW4	3.94	100	1.51	7
23	DOW4	0.95	120	0.76	8
24	DOW4	0.99	120	3.00	6
B0	none	0.00	120	1.51	8

Table 4.3: Measures from the reactor loading step of experiment 15.

Experiment ID: 15 Catalyst: DOW4		Date: 2nd November 2016	
Reaction vessel, empty; $m_{rv,em}$	1 535.34 g	Fructose; $m_{fr,0}$	1.503 g
BuOH cylinder, full; $m_{Bu,cyl,fu}$	188.94 g	Water cylinder, full; $m_{w,cyl,fu}$	61.38 g
BuOH cylinder, empty; $m_{Bu,cyl,em}$	141.27 g	Water cylinder, empty; $m_{w,cyl,em}$	51.66 g
Reaction vessel, full; $m_{rv,fu,0}$	1 594.17 g	Catalyst; $\hat{m}_{cat}$	1.017 g
Catalyst funnel, unclean; $m_{fn,di}$	2.413 g	Catalyst watch glass, unclean; $m_{wg,di}$	24.552 g
Catalyst funnel, clean; m_{fn}	2.388 g	Catalyst watch glass, clean; m_{wg}	24.542 g
Reaction vessel, full (end); $m_{rv,fu}$	1 583.96 g	Volume recovered; $\hat{V}_T$	51 mL

Table 4.4: List of molecular masses and densities of substances of interest for this work [32].

j	$M_j/(\mathrm{g/mol})$	$\rho_j/(\mathrm{g/L})$
Butan-1-ol	74.12	0.81
5-(Butoxymethyl)furfural	182.22	—
Butyl formate	102.13	0.89
Butyl levulinate	172.22	0.97
Di-*n*-butyl ether	130.23	0.77
Formic acid	46.02	1.22
D-Fructose	180.16	1.69
5-(Hydroxymethyl)furfural	126.11	1.29
Levulinic acid	116.11	1.14
Water	18.01	1.00

- Initial mass of water: $m_{\mathrm{w},0} = m_{\mathrm{w,cyl,fu}} - m_{\mathrm{w,cyl,em}}$
- Mass of catalyst: $m_{\mathrm{cat}} = \hat{m}_{\mathrm{cat}} - (m_{\mathrm{fn,di}} - m_{\mathrm{fn}}) - (m_{\mathrm{wg,di}} - m_{\mathrm{wg}})$
- Total initial mass (excluding catalyst): $m_{\mathrm{T},0} = m_{\mathrm{fr},0} + m_{\mathrm{Bu},0} + m_{\mathrm{w},0}$
- Initial mass fraction of component j: $w_{j,0} = m_{j,0}/m_{\mathrm{T},0}$

Now, knowing the molecular mass M_j of each compound j,[(3)] these quantities can be transformed into moles and mole fractions:

- Initial moles of component j: $n_{j,0} = m_{j,0}M_j$
- Total initial moles (excluding catalyst): $n_{\mathrm{T},0} = \sum_j n_{j,0}$
- Initial mole fraction of component j: $x_{j,0} = n_{j,0}/n_{\mathrm{T},0}$

The results of all these operations can be seen in Table 4.5.

4.5.2 Contraction coefficients

The results of the chromatographic analysis can be converted directly into concentrations by means of the calibration curves, visible in § 4.5.3. Nevertheless, this conversion is made in relation to the reaction volume. Due to mass losses in the sampling process, among other causes,

[(3)] V. Table 4.4 for a list of molecular masses of interest for this work.

Table 4.5: Results of the reactor loading step.

Mass results		Mole results	
$m_{Bu,0}$	47.67 g	$n_{Bu,0}$	0.643 mol
$m_{w,0}$	9.72 g	$n_{w,0}$	0.540 mol
m_{cat}	0.98 g	$n_{fr,0}$	0.008 mol
$m_{T,0}$	58.89 g	$n_{T,0}$	1.191 mol
$w_{Bu,0}$	80.94 %	$x_{Bu,0}$	53.99 %
$w_{w,0}$	16.50 %	$x_{w,0}$	45.31 %
$w_{fr,0}$	2.55 %	$x_{fr,0}$	0.70 %

this reaction volume is not constant, and this issue must be reflected in the calculations: at different times, the conversion of the chromatographic data into concentrations will be done taking different volumes. This phenomenon can be modelled using a mass contraction coefficient, $\dot{m}$, and a volume contraction coefficient, $\dot{V}$.

The first step to obtain these contraction coefficients is to calculate the density of the reaction mixture at the end of the reaction. Since the recovered volume and mass are known (v. Table 4.3), its density is simply

$$\rho = \frac{\hat{m}_T}{\hat{V}_T}$$

where $\hat{m}_T$ can be determined as $m_{rv,fu} - m_{rv,em} - m_{cat}$. Nevertheless, if a number N_{sm} of samples is taken throughout the process with an average volume $\bar{V}_{sm}$, there will be a volume $N_{sm}\bar{V}_{sm}$ lacking from the final reaction mixture that ought to be considered. The true total final mass will hence be

$$m_T = \hat{m}_T + \rho N_{sm}\bar{V}_{sm}$$

The mass contraction coefficient will then be defined as

$$\dot{m} = \frac{m_T - m_{T,0}}{t}$$

For the volume contraction coefficient, a similar reasoning can be used. Assuming additive volumes, the initial total volume of the reaction mixture can be calculated as

$$V_{T,0} = \frac{m_{Bu,0}}{\rho_{Bu}} + \frac{m_{w,0}}{\rho_w} + \frac{m_{fr,0}}{\rho_{fr}}$$

On the other side, analogically to what happened with the mass, $\hat{V}_T$ does not take into account the sampling volume that has been drawn from the system. The true total final volume will hence be

$$V_T = \hat{V}_T + N_{sm}\bar{V}_{sm}$$

Table 4.6: Results of the contraction coefficients.

Mass results		Volume results	
ρ	0.93 g/mL	$V_{T,0}$	68.57 mL
m_T	52.31 g	V_T	56.00 mL
$\dot{m}$	−0.82 g/h	$\dot{V}$	−1.57 mL/h

The volume contraction coefficient will then be defined as

$$\dot{V} = \frac{V_T - V_{T,0}}{t}$$

The results of all these operations can be seen in Table 4.6. With them, the total mass and volume of reaction (always excluding the catalyst) at the instant t are determined by:

$$m_{T,t} = m_{T,0} + \dot{m}t$$

$$V_{T,t} = V_{T,0} + \dot{V}t$$

4.5.3 Chromatographic measurements

The results of the chromatographic analyses are given in terms of peak areas (HPLC) or peak area percentages (GC), which will be denoted by $A_{j,t}$ for a compound j at an instant t. These measurements can be translated into concentrations by means of a calibration equation of the form $C_{j,t} = \alpha_j + \beta_j A_{j,t}$ where α_j and β_j are the calibration coefficients for the compound j, which can be seen in Table 4.7.

Once converted, GC results are given in mass fraction and HPLC results are given in mass concentration (grammes per litre). These can be transformed into moles as follows. For mass

Table 4.7: Coefficients for the calibration equations [32].

Gas chromatography			High-pressure liquid chromatography		
Compound j	α_j	β_j	Compound j	α_j	β_j
Butan-1-ol	-2.477×10^{-2}	9.827×10^{-3}	Formic acid	1.734×10^{-3}	9.602×10^{-6}
5-BMF	3.234×10^{-3}	1.147×10^{-2}	Fructose	-5.542×10^{-3}	3.471×10^{-6}
Butyl form.	3.916×10^{-3}	1.108×10^{-2}	5-HMF	3.061×10^{-3}	2.902×10^{-6}
Butyl levul.	3.234×10^{-3}	1.147×10^{-2}	Levul. acid	-4.236×10^{-2}	5.253×10^{-6}
Dibutyl eth.	-1.018×10^{-4}	9.422×10^{-3}			
Water	2.808	8.826×10^{-1}			

fractions:

$$n_{j,t} = \frac{w_{j,t} m_{\mathrm{T},t}}{M_j}$$

For mass concentrations:

$$n_{j,t} = \frac{C_{j,t} V_{\mathrm{T},t}}{M_j}$$

being careful enough to convert $V_{\mathrm{T},t}$, which is usually expressed in millilitres, into litres.

Once these amounts have been determined, the calculation of conversions, selectivities and yields is rather straightforward. The conversion of fructose at an instant t is given by

$$X_{\mathrm{fr},t} = \frac{n_{\mathrm{fr},0} - n_{\mathrm{fr},t}}{n_{\mathrm{fr},0}}$$

The selectivity of a substance j over fructose at an instant t can be calculated through

$$S_{j,t} = \frac{n_{j,t}}{n_{\mathrm{fr},0} - n_{\mathrm{fr},t}}$$

without the need of a stoichiometric coefficient, since all reactions have got 1:1 stoichiometry. Finally, the yield of a substance j at an instant t is given by

$$Y_{j,t} = S_{j,t} X_{\mathrm{fr},t}$$

4.5.4 Observational error

There are two experiments that were replicated three times each: catalyst DOW2 with 1.5 g of fructose at 120 °C (experiments 4, 8 and 13) and catalyst DOW4 with 1.5 g of fructose at 120 °C (experiments 7, 14 and 15). This was done in order to determine the observational error of the measurements. A 95 % confidence interval was chosen for its being the most commonly used [38]. Working with the number of moles of a substance j at an instant t, the average number of moles for three replicates is calculated as

$$\bar{n}_{j,t} = \frac{\sum_{i=1}^{3} n_{j,t,i}}{3}$$

and the standard deviation of the measurement will be defined as

$$s_{j,t} = \sqrt{\frac{1}{3-1} \sum_{i=1}^{3} (n_{j,t,i} - \bar{n}_{j,t})^2}$$

If three replicates were made, the 95 % confidence limits will be determined by

$$\bar{n}_{j,t} \pm \frac{s_{j,t}}{\sqrt{3}}$$

In this equation, for only three replicates, a very high Student's *t*-value would apply (only two degrees of freedom); nevertheless, this would imply extremely high error values that would render its determination useless. Therefore, the equation will be applied directly as shown above.

5 Results and discussion

5.1 Blank experiment

A blank experiment, i.e. an experiment without any catalyst, was performed as a reference point to assess the usefulness of heterogeneous catalysis for this reaction. Figure 5.1 shows the output of this experiment. It can be seen that very little fructose reacts and only a small amount of 5HMF is generated. No other compounds are observed.

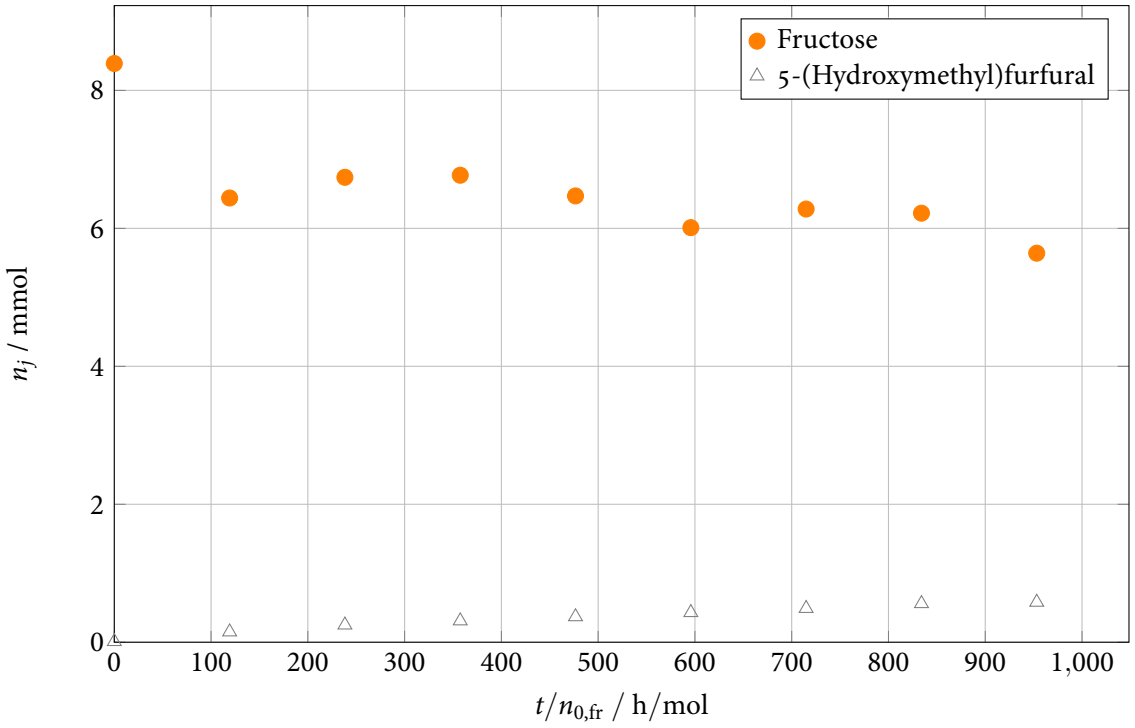

Figure 5.1: Output of an experiment without catalyst, experiment BO.

5.2 Output of a typical experiment

Figure 5.2 depicts the average output of experiments 7, 14 and 15. All three of them were carried out with around 1 g of DOW4 and 1.5 g of fructose, running for 8 h at 120 °C. All data have been plotted against a standardised time $m_{cat}t/n_{0,fr}$, which makes them independent of the mass of catalyst and the initial amount of fructose.

Three different tendencies can be clearly distinguished. Fructose, as the raw material, tends to decrease exponentially. This trend is somewhat compensated by a rapid increase of the amount of 5-HMF, peaking during the first instants of the reaction and decreasing thereafter. These tendencies confirm the reaction scheme seen in Figure 2.2, where 5-HMF is the first substance produced and then decomposes rapidly into LA and FA or 5-BMF. Also, 5-BMF can be considered an interesting compound, since it can react further to form BL. In fact, it can be seen that the concentration of 5-BMF begins to decrease slightly after 600 (g · h)/mol while BL keeps building up.

It must also be noted that FA also tends to form an ester with time, butyl formate (BF). As can be seen in Figure 5.2, BF is not detected until the concentrations of its precursors (FA and 5-BMF) are high enough, from 200 (g · h)/mol on.

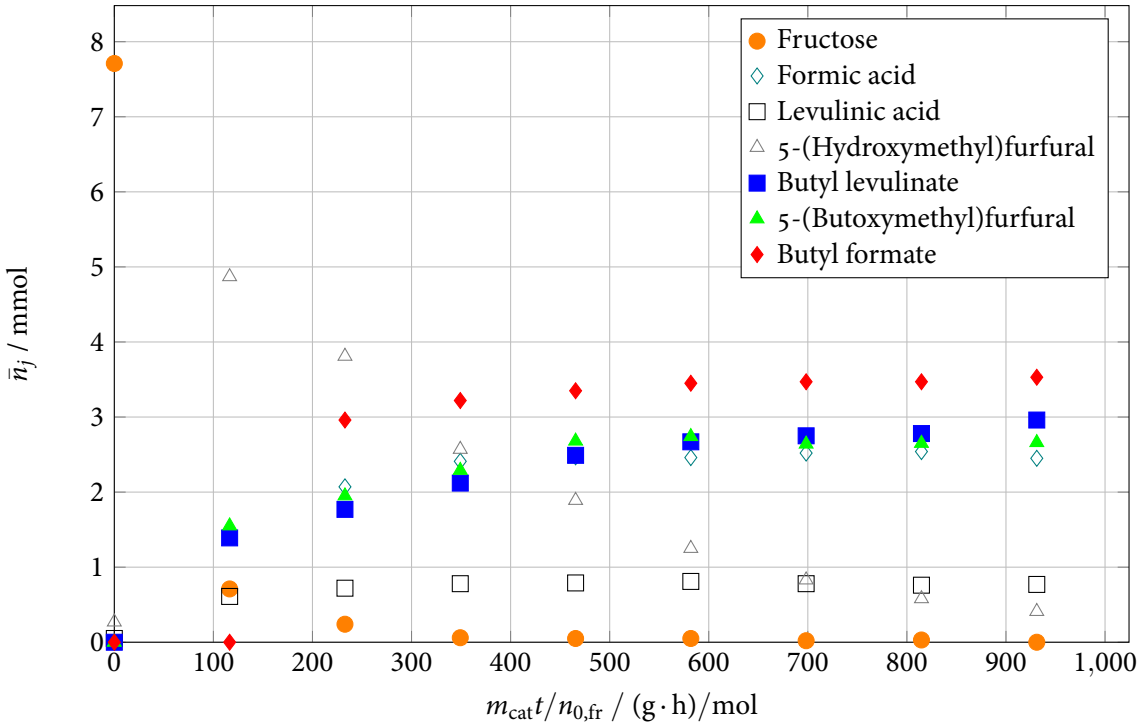

Figure 5.2: Average results of experiments 7, 14 and 15.

Although the formation of humins has been reported in the literature, such compounds were not detected in these experiments. The only sign of polymerisation was the progressive darkening of the reaction mixture, but no insoluble elements were observed. Additionally, dibutyl ether was not found either, probably thanks to the mild reaction temperature.

5.3 Experimental error

Before studying the effects of different parameters in the reaction, the experimental error had to be calculated. This measure is useful in order to determine whether or not the differences observed when changing the reaction conditions are significant.

Figure 5.3 shows the calculated experimental errors for the production of BL in experiments 7, 14 and 15. As can be seen, experimental errors are cumulative, becoming greater as the reaction progresses. The measurements at about 500 $(g \cdot h)/mol$ and 900 $(g \cdot h)/mol$ differ notably between experiments, thus increasing the uncertainty of these points. This variation, though, can be mainly attributed to experiment 7, which was among the first ones to be performed, when the experimental procedure was less perfected. The uncertainties at 900 $(g \cdot h)/mol$ are

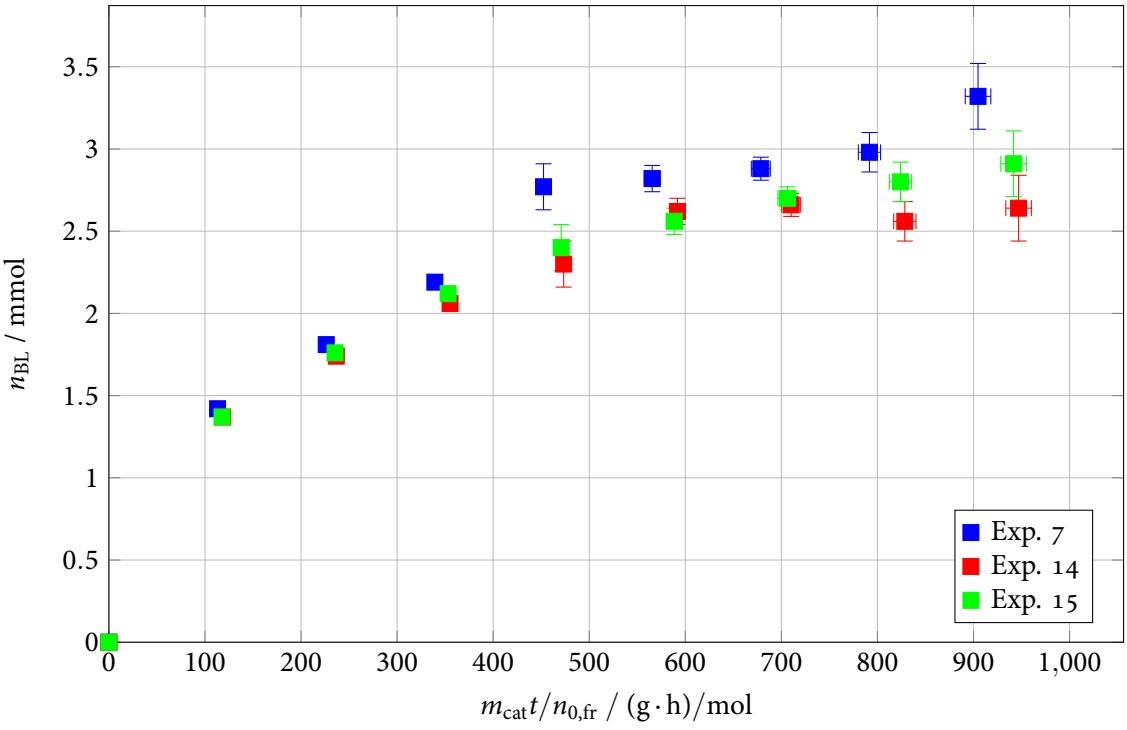

Figure 5.3: Production of BL in experiments 7, 14 and 15.

the highest, with a value of ±0.20 mmol. The uncertainty of the abscissae is a consequence of experimental error when measuring the amount of catalyst.

5.4 Catalyst screening

The screening phase of this Master's Thesis consisted on testing different catalysts in the same conditions in order to compare their outputs. In this case, experiments were performed with 1 g of catalyst and 1.5 g of fructose, running for 8 h at 120 °C.

The conversion of fructose attained high values of over 95 % in all cases, but the highest values (above 99 %) were achieved with Dowex® resins. This can be seen in Figure 5.4. The significantly lower fructose conversion with non-Dowex® catalysts led to the discardment of CT124 and A31 resins.

As for Dowex® resins, their performance is very similar in all three cases. It looks like DOW8 tends to favour LA and 5-HMF instead of their esters. Figure 5.5, for instance, shows that the selectivity towards 5-HMF is notably higher with this catalyst. The same happens with formic acid. This could be explained by its higher DVB percentage: its high degree of cross-linking

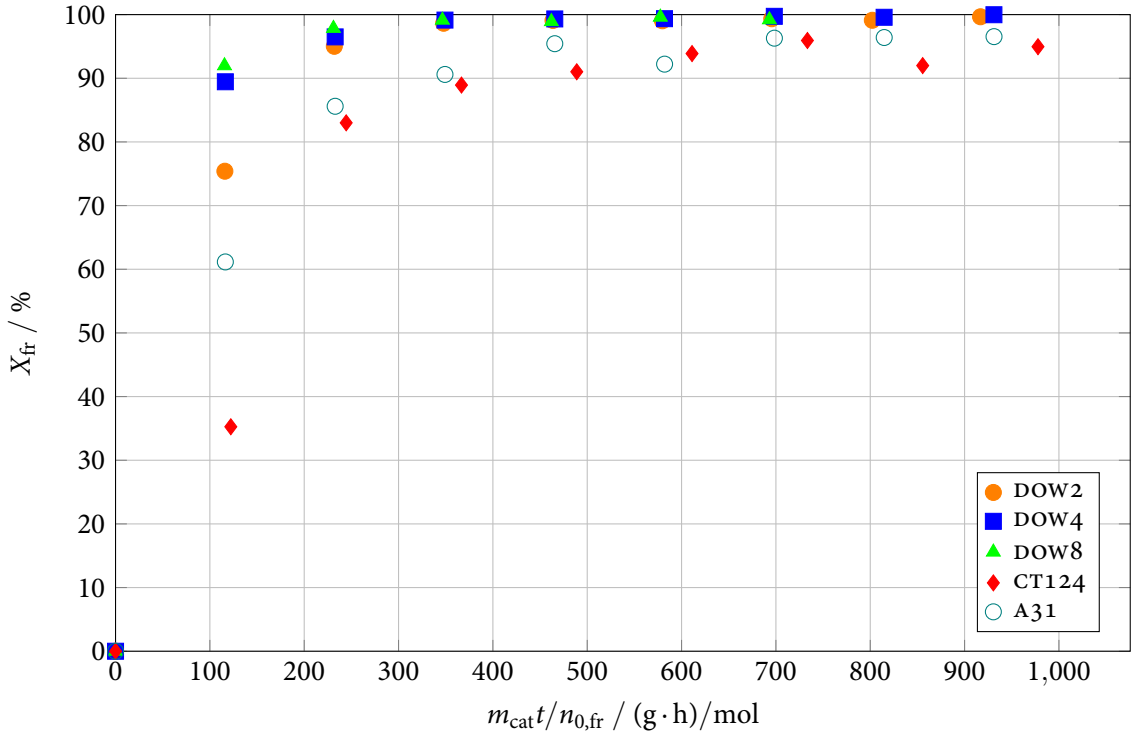

Figure 5.4: Fructose conversion with each catalyst. Conditions:1.5 g fructose, 1 g catalyst, 120 °C.

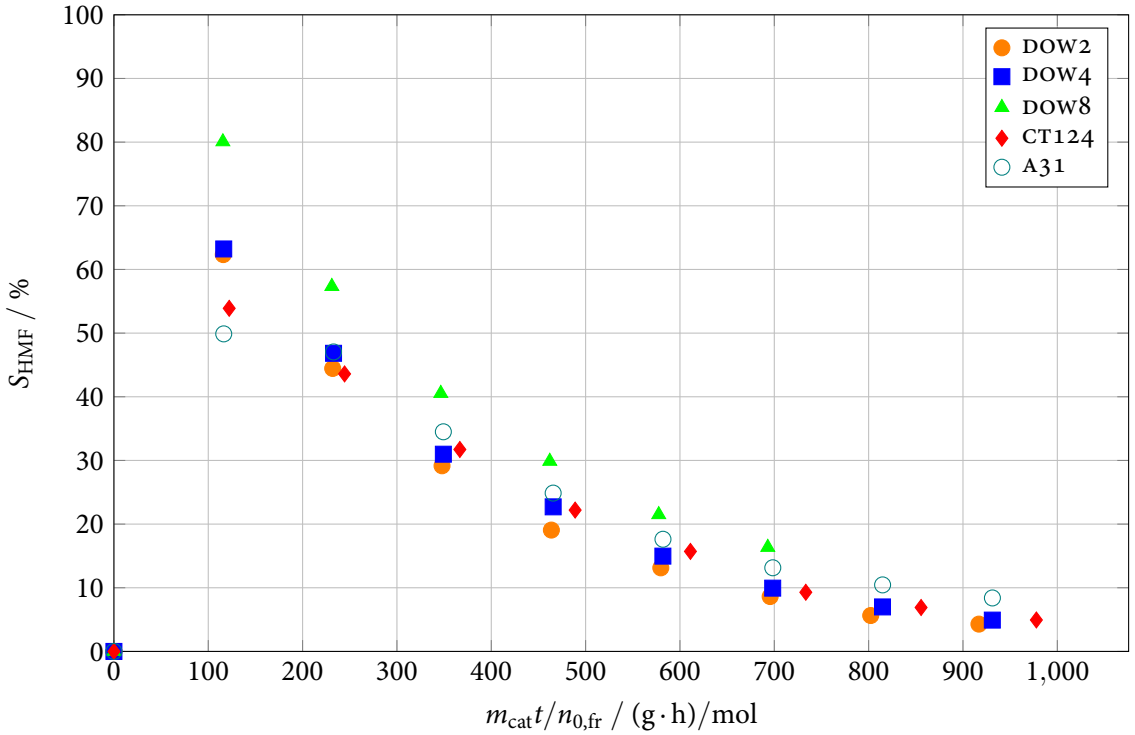

Figure 5.5: Selectivity towards 5-HMF with each catalyst. Conditions: 1.5 g fructose, 1 g catalyst, 120 °C.

only allows it to swell about half as much as the other two,[(1)] thus having an effect of steric hindrance against the ester molecules, which are larger. This interpretation agrees with previous research [5, 32]. Annexe A shows the results of ISEC analyses performed by GUILERA [39]: it can be seen that the pores generated in DOW8 after swelling, which are in the range of 1.5 nm^{-2}, are actually much smaller than in other resins, further obstructing the formation of the esters. Since the compounds of interest for this work are actually the esters, DOW8 was also discarded.

The decision between DOW2 and DOW4, though, was quite harder to make. Both catalysts have very similar performances, presumably indistinguishable when taking into account the confidence interval derived from the experimental error. Looking at the selectivity towards BL (the desired product), Figure 5.6, the performance of DOW4 is slightly better, the fructose conversion also being very slightly higher. Additionally, the higher DVB content of DOW4 could imply a higher mechanical resistance, which would be beneficial for its use in industrial applications, and its price might be scarcely lower. Taking into account these criteria, DOW4 was finally chosen over DOW2.

(1) V. Table 4.1.

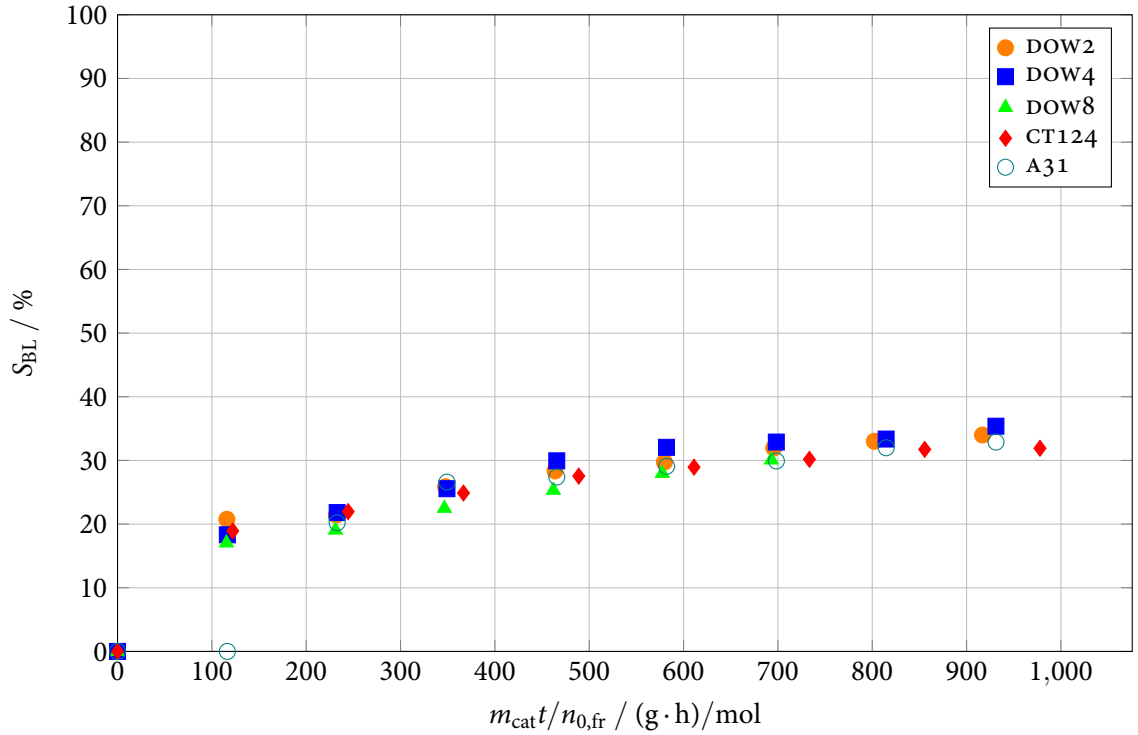

Figure 5.6: Selectivity towards BL with each catalyst. Conditions: 1.5 g fructose, 1 g catalyst, 120 °C.

5.5 Temperature variation

Once DOW4 was selected, four additional experiments were performed at 100 °C, 110 °C, 130 °C and 140 °C. Varying amounts of catalyst were used: 4 g at 100 °C, 2 g at 110 °C and 0.5 g at 130 °C and 140 °C. The reason for this was that, if the same amount of catalyst had been used, the reaction times would have been too long for the experiments at lower temperatures and too short for the experiments at higher temperatures. Since it has been proved that the mass of catalyst does not affect the results when plotting them against $m_{cat}t/n_{0,fr}$ [32], less catalyst was added at higher temperatures and vice versa.

Figure 5.7 shows that fructose conversion reaches completion at all temperatures. It has been observed that, at higher temperatures, the selectivities towards all products and by-products tend to drop slightly. This effect, visible in Figure 5.8 for BL, should be attributed to a higher loss of reaction mass at high temperatures due to stronger volatilisation. However, higher temperatures, albeit lower than the maximum design temperatures of the catalyst, might pose a threat to its integrity and imply greater operation costs, besides favouring the formation of unwanted by-products such as DBE. On the contrary, lower temperatures would need longer operation times (and hence costs) or greater amounts of catalyst. Therefore, a temperature of 120 °C was selected as ideal.

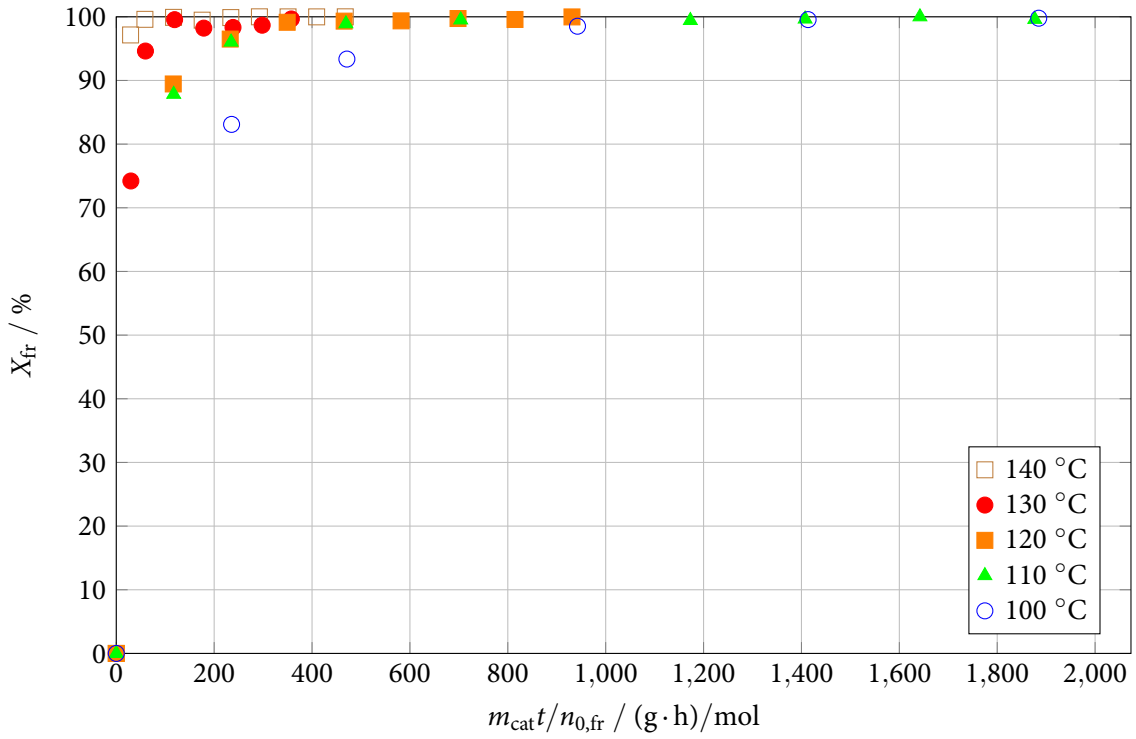

Figure 5.7: Variation on fructose conversion with temperature.

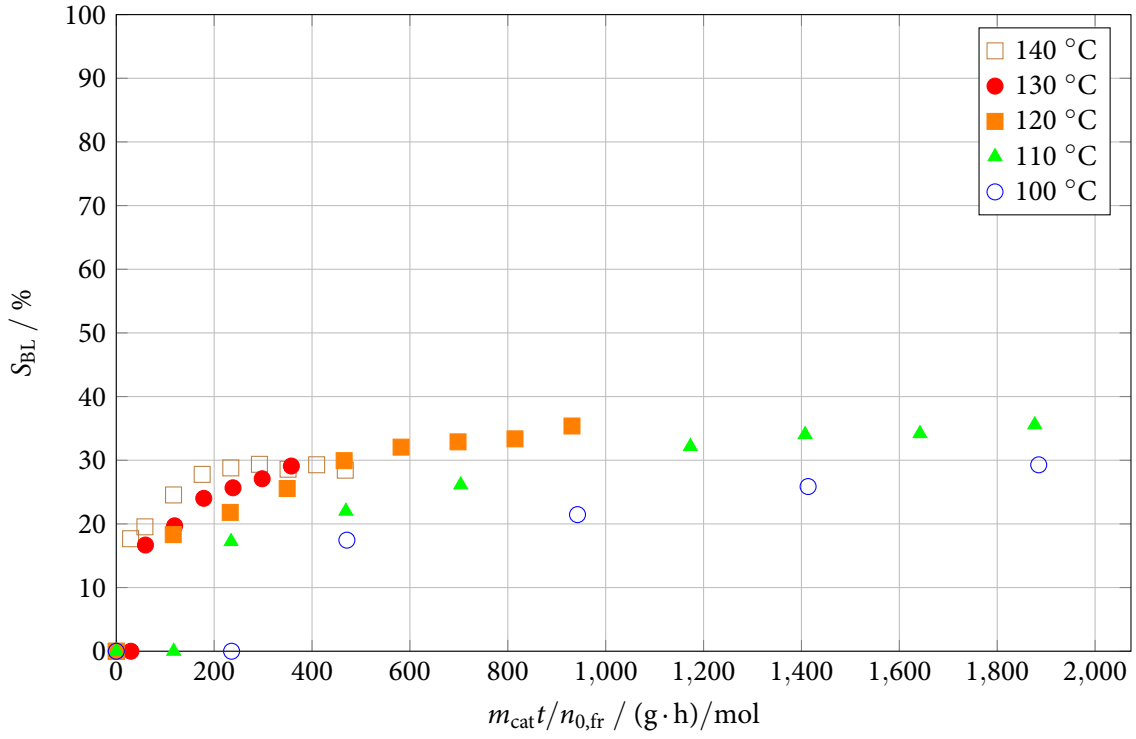

Figure 5.8: Variation on selectivity towards BL with temperature.

5.6 Feed composition

All previous experiments were performed with a feed composition of 60 mL butan-1-ol, 10 mL water and 1.5 g fructose. Nevertheless, as previously stated,[(2)] there is still room for moderate variation of these numbers. Consequently, further experiments were carried out halving and doubling, respectively, the mass of fructose in the feed (i.e. 0.75 g for experiment 23 and 3 g for experiment 24). The results can be seen in Figures 5.9 and 5.10.

Once again, fructose is completely converted in all cases and, as expected, greater amounts of fructose yield higher gross concentrations of all products. When looking at selectivities, they tend to lie roughly on the same curve, as shown in Figure 5.10. Nevertheless, this does not imply that all three cases are equivalent. Even though the selectivity with 0.75 g fructose is slightly higher, this does not compensate the fact that a lower concentration of fructose means working with more dilute solutions and, therefore, obtaining a lower amount of product per volume.

This fact may seem to advise working with fructose concentrations as high as possible; however, new issues arise in this case. With 3 g fructose, the experiment had to be concluded after only

[(2)] *supra* 4.4.

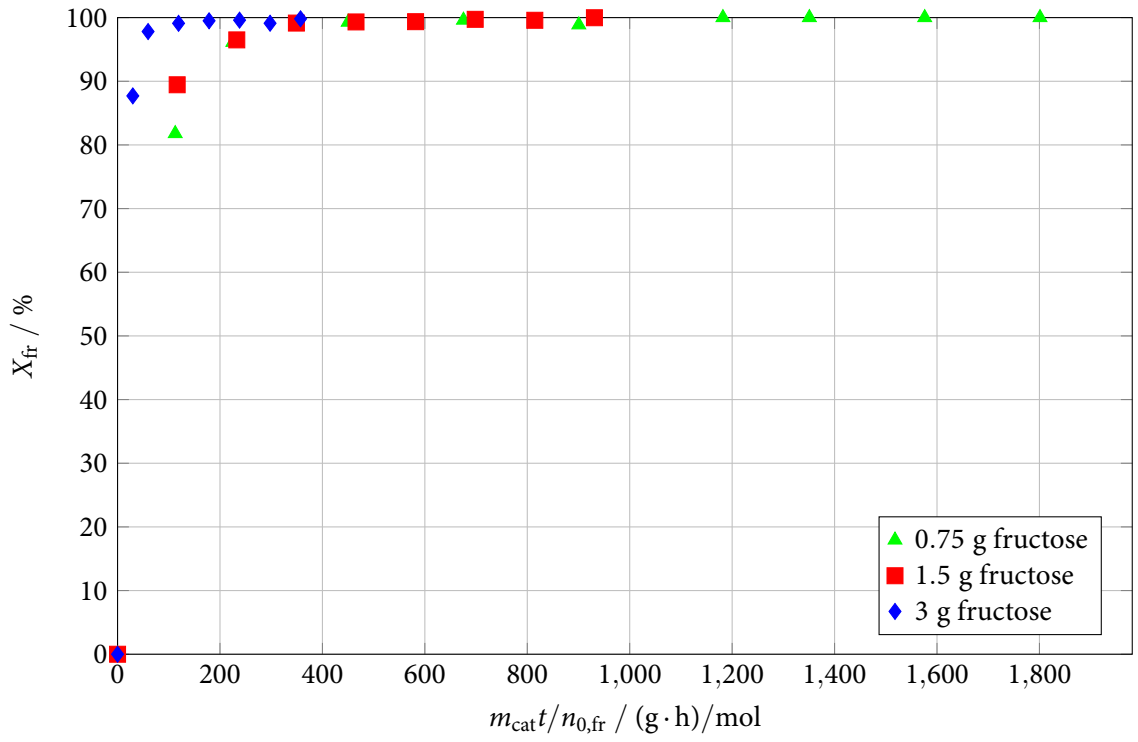

Figure 5.9: Variation on fructose conversion with mass.

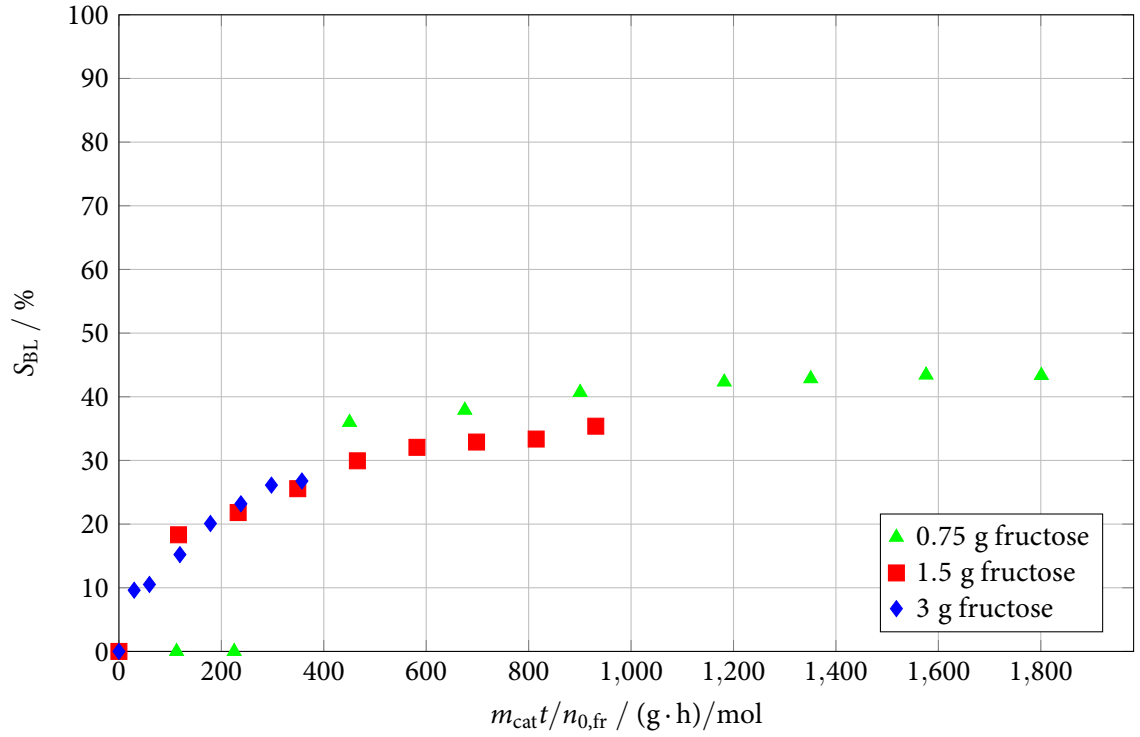

Figure 5.10: Variation on selectivity towards BL with mass of fructose.

6 h, since severe darkening of the reaction mixture was observed. This rapid darkening suggests that unwanted polymeric (albeit soluble) by-products are being created. Additionally, this was the only experiment in which the presence of DBE was reported, in samples corresponding to the last couple of hours. This suggests that an excessive amount of fructose in the feed is also inconvenient. Consequently, a mass of fructose of 1.5 g (i.e. a mass fraction of around 2.5 %) has been considered ideal. However, lacking further research, a slightly higher amount of fructose (maybe 2 g) might lead to better results.

5.7 Open questions

The experiments performed along this work have found answers to the questions posed as objectives, but they have also originated new questions that will have to be answered through further research.

One such question is the very different performance of DOW4, A31 and CT124, even though they all have got the same DVB percentage[3] and internal structure[4] and they even swell in

[3] V. Table 4.1
[4] *infra* A.1

a similar proportion in butanol. The most probable answer is that both A31 and CT124 were ground in order to obtain the same particle diameter as Dowex® resins, which may have affected their internal structure and, therefore, their performance.

It has also been observed that a loss of mass of around 10 % is lost throughout the experiments. This can be explained by volatilisation of the substances present in the reaction mixture, that would escape the system during the sampling process. This would be consistent with the fact that greater losses were measured when working at higher temperatures. Nevertheless, abnormal amounts of BF and, especially, FA were detected. This could imply the formation of undetected volatile molecules during the very first instants of the reaction, which could help to explain these losses, as well as the sharp fall in the fructose concentration in the first moments of the blank experiment (v. Figure 5.1).

6 | Conclusions

For the chain of reactions that leads from D-fructose to butyl levulinate, this study has shown that resins with a lower content of DVB, implying a lower crosslinking degree, generally perform better. An explanation for this could be that a higher DVB percentage prevents the resin from swelling, thus maintaining a smaller pore diameter. This smaller pore size would benefit 5-(hydroxymethyl)furfural and levulinic acid, producing a steric hindrance effect on their (larger) esters. It was observed that Dowex® catalysts performed notably better than A31 and CT124 and, among them, DOW4 was selected as the best. Nevertheless, DOW2 showed a very similar behaviour, and the differences between both resins might not be statistically significant. The potentially better mechanical resistance and slightly lower price of DOW4 were also taken into account for this choice.

Experiments were carried out with DOW4 at five different temperatures between 100 °C and 140 °C. It was observed that higher temperatures favour 5-(hydroxymethyl)furfural and levulinic acid over their esters. The highest yields towards BL (over 35 %) were attained at 110 °C and 120 °C.[1] Since lower temperatures would imply longer operation times or greater amounts of catalyst, 120 °C was selected as the ideal temperature.

Finally, the concentration of fructose in the feed was varied and the output analysed in order to determine the optimum composition of the initial reaction mixture. The responses of each experiment lay roughly on the same curve, as shown in Figure 5.10. Even though a yield higher than 40 % was achieved working with dilute solutions, it was considered that this would not compensate the fact that the final product gross concentration would still be significantly lower. An initial mass fraction of fructose of around 2.5 % was considered optimum, albeit mass fractions up to 3.5 % might also yield satisfactory results, lacking further research.

[1] Yield and selectivity results for long reaction times are similar, since the conversion of fructose always achieves values near 100 %.

Bibliography

[1] Northon, K. [ed.]: Nasa, Noaa Data Show 2016 Warmest Year on Record Globally. In: *Nasa* [online]. Washington, dc, 18th January 2017 [retrieved 11th February 2017]. Available in: https://goo.gl/uCy0dZ.

[2] Ellabban, O.; Abu-Rub, H.; Blaabjerg, F.: Renewable energy resources: Current status, future prospects and their enabling technology. *Renew. Sust. Energ. Rev.* 2014, **39,** 748–764. Doi: 10.1016/j.rser.2014.07.113.

[3] Eurostat: Final energy consumption by sector. In: *Energy: Main tables* [online]. Kirchberg, Luxembourg, 11th August 2016 [retrieved 11th February 2017]. Available in: https://goo.gl/1BEkDX.

[4] United States Environmental Protection Agency: *Inventory of U.S. Greenhouse Gas Emissions and Sinks: 1990–2014* [online]. 15th April 2016 [retrieved 11th February 2017]. Pdf format. Available in: https://goo.gl/QIhzgd.

[5] Tejero, M. À. et al.: Esterification of levulinic acid with butanol over ion exchange resins. *Appl. Catal. A – Gen.* 2016, **517,** 56–66. Doi: 10.1016/j.apcata.2016.02.032.

[6] Banerjee, S. et al.: Commercializing lignocellulosic bioethanol: technology bottlenecks and possible remedies. *Biofuel Bioprod. Bior.* 2010, **4**(1), 77–93. Doi: 10.1002/bbb.188.

[7] Behera, S. et al.: Scope of algae as third generation biofuels. *Front. Bioeng. Biotech.* 2015, **2,** art. 90. Doi: 10.3389/fbioe.2014.00090.

[8] Guilera, J. et al.: Comparison between Ethanol and Diethyl Carbonate as Ethylating Agents for Ethyl Octyl Ether Synthesis over Acidic Ion-Exchange Resins. *Ind. Eng. Chem. Res.* 2012, **51**(50), 16525–16530. Doi: 10.1021/ie3004978.

[9] Christensen, E. et al.: Properties and Performance of Levulinate Esters as Diesel Blend Components. *Energ. Fuel.* 2011, **25**(11), 5422–5428. Doi: 10.1021/ef201229j.

[10] Ahmad, E. et al.: Catalytic and mechanistic insights into the production of ethyl levulinate from biorenewable feedstocks. *Green Chem.* 2016, **18**(18), 4804–4823. Doi: 10.1039/c6gc01523a.

[11] Bozell, J. J.; Petersen, G. R.: Technology development for the production of biobased products from biorefinery carbohydrates—the US Department of Energy's "Top 10" revisited. *Green Chem.* 2010, **12**(4), 539–554. Doi: 10.1039/b922014c.

[12] Démolis, A.; Essayem, N.; Rataboul, F.: Synthesis and Applications of Alkyl Levulinates. *ACS Sustain. Chem. Eng.* 2014, **2**(6), 1338–1352. Doi: 10.1021/sc500082n.

[13] Conrad, M.: Ueber Acetsuccinsäureester und dessen Derivate. *Liebigs Ann. Chem.* 1877, **188**(1-2), 217–226. Doi: 10.1002/jlac.18771880111.

[14] Sah, P. P. T.; Ma, S.-Y.: Levulinic Acid and its Esters. *J. Am. Chem. Soc.* 1930, **52**(12), 4880–4883. Doi: 10.1021/ja01375a033.

[15] Schuette, H. A.; Cowley, M. A.: Levulinic Acid. II. The Vapor Pressures of its Alkyl Esters (C_1–C_6). *J. Am. Chem. Soc.* 1931, **53**(9), 3485–3489. Doi: 10.1021/ja01360a039.

[16] Patil, C. R. et al.: Esterification of levulinic acid to ethyl levulinate over bimodal micro-mesoporous H/BEA zeolite structures. *Catal. Comm.* 2014, **43,** 188–191. Doi: 10.1016/j.catcom.2013.10.006.

[17] Melero, J. A. et al.: Efficient conversion of levulinic acid into alkyl levulinates catalyzed by sulfonic mesostructured silicas. *Appl. Catal. A – Gen.* 2013, **466,** 116–122. Doi: 10.1016/j.apcata.2013.06.035.

[18] Fagan, P. J. et al.: *Preparation of levulinic acid esters and formic acid esters from biomass and olefins.* 2003. International Patent wo 03/085071 a1.

[19] Garves, K.: Acid Catalyzed Degradation of Cellulose in Alcohols. *J. Wood Chem. Technol.* 1988, **8**(1), 121–134. Doi: 10.1080/02773818808070674.

[20] Hu, X. et al.: Reaction pathways of glucose during esterification: Effects of reaction parameters on the formation of humin type polymers. *Bioresource Technol.* 2011, **102**(21), 10104–10113. Doi: 10.1016/j.biortech.2011.08.040.

[21] Hu, X. et al.: Acid-catalyzed conversion of mono- and poly-sugars into platform chemicals: Effects of molecular structure of sugar substrate. *Bioresource Technol.* 2013, **133,** 469–474. Doi: 10.1016/j.biortech.2013.01.080.

[22] Ståhlberg, T. et al.: Synthesis of 5-(Hydroxymethyl)furfural in Ionic Liquids: Paving the Way to Renewable Chemicals. *ChemSusChem.* 2011, **4**(4), 451–458. Doi: 10.1002/cssc.201000374.

[23] Saravanamurugan, S.; Riisager, A.: Zeolite Catalyzed Transformation of Carbohydrates to Alkyl Levulinates. *ChemCatChem.* 2013, **5**(7), 1754–1757. Doi: 10.1002/cctc.201300006.

[24] Peng, L.; Lin, L.; Li, H.: Extremely low sulfuric acid catalyst system for synthesis of methyl levulinate from glucose. *Ind. Crop. Prod.* 2012, **40,** 136–144. Doi: 10.1016/j.indcrop.2012.03.007.

[25] Liu, R. et al.: Conversion of fructose into 5-hydroxymethylfurfural and alkyl levulinates catalyzed by sulfonic acid-functionalized carbon materials. *Green Chem.* 2013, **15**(10), 2895–2903. Doi: 10.1039/c3gc41139g.

[26] Peng, L. et al.: Conversion of carbohydrates biomass into levulinate esters using heterogeneous catalysts. *Appl. Energ.* 2011, **88**(12), 4590–4596. Doi: 10.1016/j.apenergy.2011.05.049.

[27] Tominaga, K.: *Method for producing levulinic acid ester.* 2006. Japan: patent jp2006-206579.

[28] Hu, X.; Li, C.-Z.: Levulinic esters from the acid-catalysed reactions of sugars and alcohols as part of a bio-refinery. *Green Chem.* 2011, **13**(7), 1676–1679. Doi: 10.1039/C1GC15272F.

[29] Lourvanij, K.; Rorrer, G. L.: Dehydration of glucose to organic acids in microporous pillared clay catalysts. *Appl. Catal. A – Gen.* 1994, **109**(1), 147–165. Doi: 10.1016/0926-860X(94)85008-9.

[30] Corain, B.; Zecca, M.; Jeřábek, K.: Catalysis and polymer networks — the role of morphology and molecular accessibility. *J. Mol. Catal. A – Chem.* 2001, **177**(1), 3–20. Doi: 10.1016/S1381-1169(01)00305-3.

[31] Schlick, S.; Bortel, E.; Dyrek, K.: Catalysis on polymer supports. *Acta Polym.* 1996, **47**(1), 1–15. Doi: 10.1002/actp.1996.010470101.

[32] Sharma, R.: *A contribution to the study of acidic ion-exchange resins to produce butyl levulinate from fructose and butyl alcohol* [Bachelor's Thesis]. 2016. Barcelona, Spain: University of Barcelona. Uri: http://hdl.handle.net/2445/101677.

[33] Tejero Iborra, M. À.: *A contribution to the study of butyl levulinate synthesis in the liquid-phase on ion-exchange resins* [Bachelor's Thesis]. 2015. Barcelona, Spain: University of Barcelona. Uri: http://hdl.handle.net/2445/67243.

[34] Góral, M.; Wiśniewska-Gocłowska, B.; Mączyński, A.: Recommended Liquid-Liquid Equilibrium Data. Part 4. 1-Alkanol–Water Systems. *J. Phys. Chem. Ref. Data.* 2006, **35**(3), 1391–1414. Doi: 10.1063/1.2203354.

[35] Jackson, R. F.; Silsbee, C. G.; Proffitt, M. J.: The preparation of levulose. *Sci. Pap. Bur. Stand.* 1926, **20,** 587–617. Doi: 10.6028/nbsscipaper.209.

[36] Young, F. E.; Jones, F. T.; Lewis, H. J.: D-Fructose–Water Phase Diagram. *J. Phys. Chem. – us.* 1952, **56**(9), 1093–1096. Doi: 10.1021/j150501a015.

[37] Oudshoorn, A. et al.: Exploring the potential of recovering 1-butanol from aqueous solutions by liquid demixing upon addition of carbohydrates or salts. *J. Chem. Technol. Biot.* 2011, **86**(5), 714–718. Doi: 10.1002/jctb.2577.

[38] Filliben, J. J.; Heckert, N. A.: Exploratory Data Analysis: 1.3.5.2. Confidence Limits for the Mean. In Croarkin, C.; Tobias, P. [eds.]: *Engineering Statistics Handbook* [online]. Gaithersburg, md: National Institute of Standards and Technology, 2003 [retrieved 15th February 2017]. Available in: https://goo.gl/dRbi7w.

[39] Guilera Sala, J.: *Ethyl octyl ether synthesis from 1-octanol and ethanol or diethyl carbonate on acidic ion-exchange resins* [Doctoral Thesis]. 2013. Barcelona, Spain: University of Barcelona. Uri: http://hdl.handle.net/2445/45985.

[40] Ogston, A. G.: The spaces in a uniform random suspension of fibres. *T. Faraday Soc.* 1958, **54,** 1754–1757. Doi: 10.1039/TF9585401754.

Annexes

Annexe A | Resins' internal structure

This Annexe aims to illustrate the internal structure of the different resins used throughout this work. When gel-type resins swell, non-permanent pores appear that can be described as spaces between rigid rods. This model was developed by Ogston [40] and has got, as a characteristic parameter, the specific volume of the swollen polymer, V_{sp}. This model is able to distinguish zones of swollen gel-phase of different polymer chain concentrations, which can be expressed as total rod length per volume unit of swollen polymer, measured in nm^{-2}.

It can be seen that DOW2 is more sparse, with almost 2 cm^3/g of pores in the 0.2 nm^{-2} range, whilst DOW8 is notably more dense, with almost all its pores in the 0.8 nm^{-2} range. Both CT124 and A31, as well as DOW4, have got rather similar internal structures, with significant specific volumes of pores in the ranges of 0.4 nm^{-2} and 0.2 nm^{-2}.

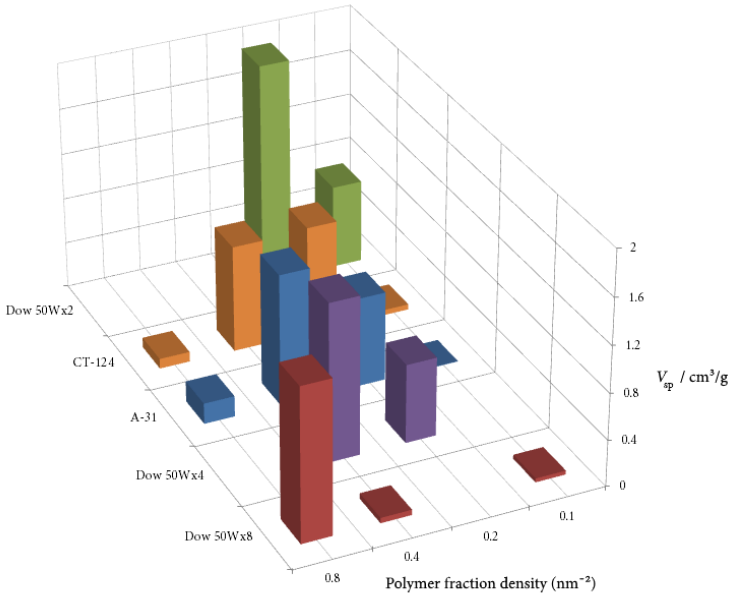

Figure A.1: ISEC pattern for gel-phase resins [39].